

Primary Radiation Defect Production in Polyethylene and Cellulose

Jussi Polvi,* Petri Luukkonen, and Kai Nordlund

Department of Physics, P.O. Box 43, FIN-00014 University of Helsinki, Finland

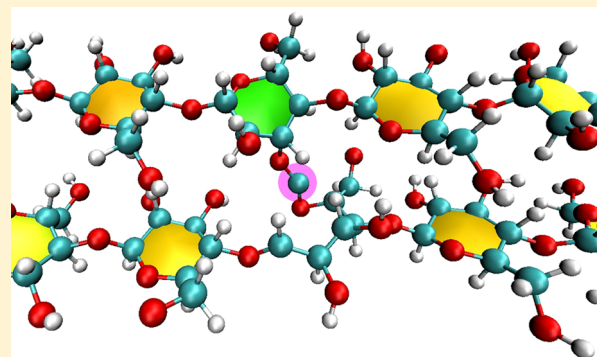
Tommi T. Järvi

Fraunhofer-Institut für Werkstoffmechanik IWM, Wöhlerstrasse 11, D-79108 Freiburg, Germany

Travis W. Kemper and Susan B. Sinnott

Department of Materials Science and Engineering, University of Florida, PO Box 116400, Gainesville, Florida 32611, United States

ABSTRACT: Irradiation effects in polyethylene and cellulose were examined using molecular dynamics simulations. The governing reactions in both materials were chain scissioning and generation of small hydrocarbon and peroxy radicals. Recombination of chain fragments and cross-linking between polymer chains were found to occur less frequently. Crystalline cellulose was found to be more resistant to radiation damage than crystalline polyethylene. Statistics on radical formation are presented and the dynamics of the formation of radiation damage discussed.



INTRODUCTION

Irradiation has been used to process and modify polymeric materials since the 1960s.¹ The earliest applications were cross-linking plastic materials, sterilizing medical equipment and preserving food products. Since then, many more practical applications for radiation-processed materials have been developed and studied. For instance, electron beam cross-linking of synthetic polymers like polyethylene can be used to produce heat-shrinkable-plastic films for packaging foods or plastic foams and hydrogels for medical applications.^{2,3}

The main reactions initiated in polymers by irradiation are polymerizing (curing), grafting, chain scissioning, and cross-linking. From the applications' point of view, cross-linking is the most important irradiation effect in polymers. This is because it can improve the mechanical and thermal properties of the polymer, thus increasing the overall chemical, environmental, and radiation stabilities of the material. Both polymer cross-linking and degradation by chain scission occur due to irradiation treatment.

The basic idea of radiation cross-linking is simple: break chains to produce smaller fragments, for example, hydrogen-deficient radicals, which act as cross-linking agents. Although radiation-induced cross-linking has been utilized in industry in a wide range of applications, some fundamental questions are still open. These questions are related to, e.g., how radicals are created near each other to induce cross-linking and how morphology influences the cross-linking reactions.^{4,5}

The most often used types of irradiation for inducing cross-linking are electrons, neutrons, and α - and β -particles with kinetic energies ranging from 100 keV to 10 MeV. Also high-energy γ - and X-rays are used with photon energies from 120 keV to 10 MeV (γ) and 100 eV to 120 keV (X-ray). Typical dose requirements for cross-linking are in the range of 50–200 kGy.³

In this article, to get insight into the atomistic mechanisms of cross-linking, we examine irradiation-induced defects in two polymeric materials, high-density polyethylene (HDPE) and cellulose I β , using molecular dynamics (MD) simulations. Polyethylene is structurally and conceptually the simplest of the organic polymers, and cellulose is one of the basic biopolymers and structural components of wood and plant fibers.⁶ From the radiation cross-linking point of view, polyethylene and cellulose have been regarded to be very different. Namely, HDPE has been observed to have a high tendency for cross-linking, while cellulose is considered primarily as a degradable polymer^{7,8} in which chain scission dominates over the formation of cross-links.³

A considerable number of experimental studies relating to radiation chemistry and physics of polyethylene^{9–13} has been published, but only few computational studies are available.¹⁴ Some recent experimental studies on the irradiation of cellulose

Received: October 9, 2012

Published: November 6, 2012

are available^{8,15–17} but none where MD-simulations would have been utilized.

METHODS

Irradiation effects in HDPE and cellulose were studied using molecular dynamics simulations¹⁸ to model primary recoil cascades in the materials. The simulations involving polyethylene were carried out with the PARCAS code.¹⁹ The interatomic interactions in polyethylene were modeled with the reactive hydrocarbon potential AIREBO,^{20,21} which is based on the reactive potential model REBO, developed by Brenner.²² In addition it includes bond-order-dependent torsional and intermolecular potentials.

For cellulose simulations involving oxygen, we used the REBO potential for C, H, and O interactions by Ni et al.²³ that was recently improved and updated by Kemper and Sinnott.²⁴ These simulations were carried out using a MD code written by Travis Kemper, the same code that was used in ref 24.

Often irradiation of materials is simulated as a bombardment by a high-energy particle, like argon or deuteron, into the surface of the specimen. For example in the work of Beardmore et al.¹⁴ HDPE was bombarded by argon atoms with an energy of 1 keV. In that simulation the incident direction of the argon atom was chosen to be 60° off the surface normal in order to prevent the atom from passing through the lattice without interaction.

Another way to simulate the interaction between, e.g., the colliding electron and the lattice atom is by giving an initial kinetic energy, the recoil energy, to some randomly chosen atom (recoil atom) in the lattice. This method was used in this work. The direction of each collision, i.e., the direction of the initial velocity, was also generated randomly. This approach is suitable when one is not interested in sputtering or damage occurring at the surface and when the concentration of ions in the specimen is small enough not to have a notable effect on the chemistry of the material.

Two types of simulations were carried out for both materials: single impacts and cumulative bombardments.

For polyethylene, 10 single-impact simulations were carried out per recoil energies of 5, 10, 20, and 30 eV and 100 simulations for recoil energies of 50 and 100 eV. Each simulation was run for 10 ps to give the system some time to relax, and for all interesting reactions (like chain scissioning, free radical formation, cross-linking) time to happen. Also 100 sets of cumulative bombardments (10 consecutive impacts for each system) were carried out using a recoil energy of 100 eV. In the cumulative bombardments, each recoil simulation was 8 ps long. Between each recoil the system was briefly relaxed and cooled down with the temperature control applied to all atoms and including Berendsen pressure control, with a time constant of 200 fs.

For cellulose, 100 single-impact simulations were carried out with recoil energies of 10, 20, 30, 50, and 100 eV, and 100 sets of cumulative bombardments were carried out recoil energies of 50 and 100 eV. Because of the more complex structure of the cellulose molecule (in comparison to polyethylene) we used a longer simulation time of 20 ps.

In all simulations, the target crystal was relaxed at 0 K before the recoil event. Periodic boundary conditions were used in all directions. During irradiation, Berendsen temperature control²⁵ was applied at the cell borders (thickness 3 Å) to scale the temperature there toward 0 K.

In the polyethylene simulations only carbon atoms—and in the cellulose simulations only carbon and oxygen atoms—were chosen as recoil atoms. This was done because the mass of hydrogen is relatively small, and with higher energies, say 100 eV, hydrogen atoms can be pushed over the borders of the simulation box very easily.

To obtain information about the size distribution of free radicals and broken polymer chains, we used a clustering algorithm developed in our group, where the atoms were grouped to fragments based on a cutoff distance, which takes into account the bond lengths between different atom types and periodic boundary conditions.

RESULTS

Polyethylene. For polyethylene simulations, an orthorhombic HDPE crystal was used as the target. The size of the system was $4 \times 7 \times 16$ unit cells, with dimensions of $x = 2.9$ nm, $y = 3.6$ nm, and $z = 4.1$ nm such that the simulation cell consisted of roughly 5400 atoms. Irradiation of this system with 10 eV of energy corresponds to a 38-kGy dose of ionizing radiation.

Single-Impact Simulations. Table I shows the different kinds of radicals formed in the single-impact simulations at the

Table I. Broken Chains and Free Radicals/Saturated Molecules Formed in HDPE with Different Recoil Energies of Randomly Chosen Carbon Atoms in Single-Impact Simulations^a

E_{rec} [eV]	no. sims	1 broken chain	2 broken chains	free molecules	cross-links
5	10	0.0	0.0	0.0	0.0
10	10	0.1	0.0	0.0	0.0
20	10	0.5	0.0	0.0	0.0
30	10	0.6	0.0	0.1	0.0
50	100	0.94	0.03	0.64	0.01
100	100	0.78	0.22	1.9	0.02

^aThe reported values are the average number of incidents per one simulation.

different energies. With an energy of 5 eV, no bond breaking occurred. At 10 and 20 eV, irradiation only caused broken polyethylene chains (chain scission), as the recoil atom always remained covalently bound to its initial chain. Thus, no free radicals were generated with energies up to 20 eV.

In our simulation model, the threshold displacement energy, i.e., the smallest energy required to make a stable defect in polyethylene, is about 10 eV. This is in fair agreement with transmission electron microscope experiments, according to which the electron energy needed to induce defects in polyethylene is about 100 keV.²⁶ This corresponds to a maximal energy transfer of 20 eV to a carbon atom.

When the recoil energy is increased, we start to get more free radicals in the irradiated system. For the higher recoil energies of 50 and 100 eV, we performed more simulations to improve the statistics on free radical production and to increase the chance of cross-linking.

At the recoil energy of 50 eV, we observed chain scission in 97% of the simulations. In 3 cases out of 100, we did not predict the formation of broken chains, and in 3 simulation cases the recoil atom caused two broken chains. For recoil energies of 100 eV the target chain was broken in all cases. In 78% of the simulations a single chain was broken, and in 22%

two chains were broken. Even with the highest kinetic energy, the recoiling atom usually moves only near its nearest-neighbor chains. This means that the kinetic energy is lost quite effectively into the first neighbor chains, resulting in only one or two broken chains.

Cross-linking was observed in only one of the 50 eV simulations and in two of the 100 eV simulations. It has been proposed that in the crystalline HDPE the length of the carbon–carbon bond, ca. 1.54 Å, is too short as compared to the distance of adjacent chains 4.1 Å to allow effective cross-linking,⁵ and our observations seem to support that assumption.

The production of free radicals and other molecules in 50 and 100 eV simulations is shown in Figure 1. The most

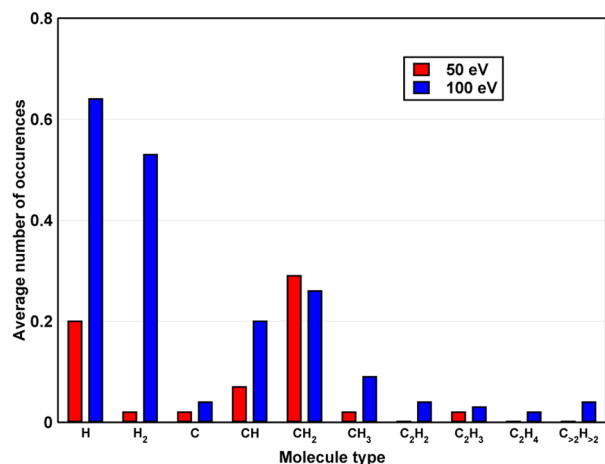


Figure 1. Average number of different types of free radicals per one simulation calculated after the single-impact simulations of polyethylene with 50- and 100-eV recoil energies.

abundant radical types are H and CH₂. The 100-eV recoils produced almost three times more free radicals and molecules than the 50-eV recoils, namely, 1.9 vs 0.64 radicals per recoil. This difference is mostly due to the large increase in the amount of atomic and molecular hydrogen.

Closer analysis of the simulations reveals the radical formation happens during the first 1 ps, and possible recombination occurs during the next 3 ps of the simulations. After that the temperature of the system has cooled down to roughly 20 K (100 eV recoils) or less, and for the rest of the simulation time the system composition is typically unchanging.

Cumulative Bombardment. The effect of higher irradiation fluences was investigated by carrying out 100 sets of cumulative bombardment trajectories as explained above. In these simulations polyethylene was exposed to 10 consecutive collisions: a randomly chosen carbon atom was given a 100-eV recoil energy, the total sequence corresponding to a dose of 3.8 MGy. After each recoil, the simulation box was relaxed to 0 K before the next recoil simulation.

Figure 2 shows the average distribution of free radicals and other molecules after 10 consecutive impacts with 100-eV recoil energy.

Obviously, multiple impacts result in more damage to the crystal structure than single impacts. From Figure 2, it can be seen that the biggest group of free radicals and molecules are atomic and molecular hydrogen with average amounts of 5.2 for H and 6.5 for H₂. (In single-impact simulations H were slightly more abundant than H₂ with $N(\text{H}) = 0.64$ and $N(\text{H}_2) = 0.53$.)

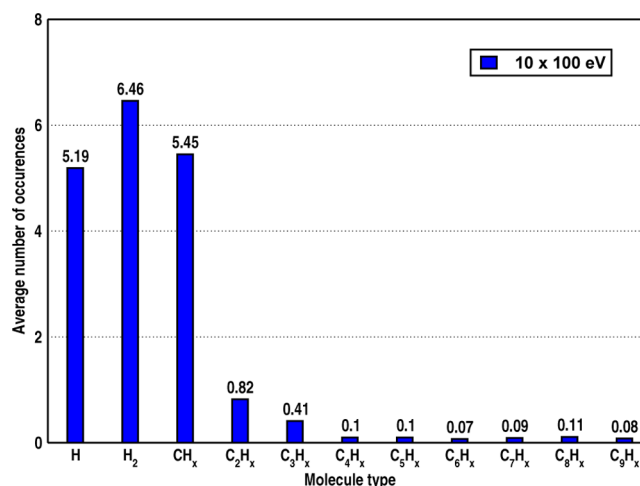


Figure 2. Average distribution of free radicals and other molecules in polyethylene after 10 consecutive recoils with 100 eV of energy.

Then come radicals of the form CH_x (where $x = 0.3$) with an average 5.16 occurrences. The rest of the bar height consists of methane molecules CH₄ with average amount of 0.29 per simulation set.

Less common are radicals with two carbon atoms, on average 0.82 molecules, and radicals with three carbon atoms, on average 0.41 molecules per simulation set. Radicals with four or more carbon atoms were found to be equally common, on roughly 0.1 molecules per simulation set. These larger molecules are not produced in the single recoil events but are formed when a new recoil hits a previously broken chain and a large fragment of the chain is broken loose.

The average number of cross-links per simulation set was 0.2, i.e., 2% of the recoils caused cross-links to form. This is, within the statistical uncertainty, the same probability for cross-linking we observed in the single-impact simulations. This seems to indicate that cumulative bombardment does not increase the occurrence of cross-links in HDPE. This is in accordance with the simulation results of Beardmore et al.,¹⁴ where they found no evidence that multiple impacts with 1 keV argon would have increased cross chain linking.

Altogether, after 10 recoil events, 16% of the polymer chains in all simulation systems were broken, meaning on average 9.0 broken chains per simulation set. In each simulation set there were on average 1.7 polymer chains that were broken into three or more pieces.

To accelerate thermally activated processes, we randomly chose 10 systems from the end states of the 100 cumulative simulation sets, which we heated up to 500 K for 40 ps. No cross-linking was observed during this annealing phase. The mobility of fragments generated by the impacts depends greatly on their size. By analysis of the simulation trajectories we observed that radicals containing two or more carbon atoms are able to pass by only one neighbor chain during the 40 ps of annealing.

The combination of radicals during the annealing was quite rare. The biggest changes in molecular distribution occurs as atomic hydrogens recombine with each other and hydrocarbon radicals, increasing the number of H₂ from 4.9 to 5.9 (20% increase) and the number of CH₂ from 1.2 to 1.8.

Cellulose. In the case of cellulose, the target in the Iβ phase was chosen. The crystal structure was constructed using coordinates provided by Nishiyama et al.²⁷ The unit cell of

the cellulose I β crystal has dimensions $a = 7.78 \text{ \AA}$, $b = 8.20 \text{ \AA}$, and $c = 10.38 \text{ \AA}$. The unit cell is not quite rectangular but has a 96.55° angle between the a and b axes. The constructed rectangular simulation cell had dimensions of $x = 3.3 \text{ nm}$, $y = 3.5 \text{ nm}$, and $z = 3.1 \text{ nm}$ and comprised of 4032 atoms. The average distance between cellulose chains was roughly 4–5 \AA . Irradiation of this system with 10 eV of energy corresponds to a 31-kGy dose of ionizing radiation.

Because the interatomic potential contains no Coulombic interactions, we do not expect hydrogen bonding between the cellulose chains to be perfectly reproduced. Upon irradiation and annealing hydrogen bonds were seen to reorganize somewhat, but as we concentrate on the breaking of the strong covalent bonds within the lattice, we will ignore this point in the discussion below.

Single-Impact Simulations. As in the case of polyethylene, single-impact simulations were carried out to study the kinds of radicals and damage produced and whether any cross-linking would occur. To ensure significant statistics of the effect of irradiation in different parts of the cellulose monomeric unit, we increased the minimum number of single-impact simulations to 100. Half of the recoil atoms used in simulations were carbon and the other half oxygen.

As can be seen from Figure 3, in the case of cellulose, it is not necessary to break the whole chain to form reactive centers.

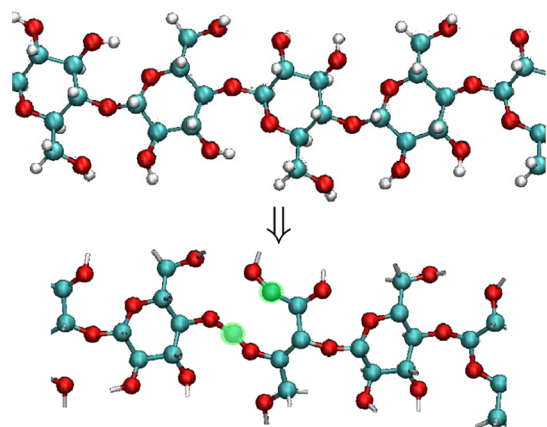


Figure 3. A cellulose chain with a broken glucose ring caused by a recoil energy of 10 eV with carbon being the recoil atom. The reactive carbon atoms are marked with green.

The cellulose chain has branches attached into its D-glucose ring which can become reactive upon irradiation. This kind of damage to the target chain was found to be very typical with simulations using recoil energies higher than 10 eV.

Table II indicates the amount of broken chains, broken D-glucose rings, and free radicals and molecules formed in cellulose in single-impact simulations. By use of a 10-eV recoil energy, we observed no other form of damage in the target chain except for a broken D-glucose ring in 5% of the simulations. These were all caused by C recoils breaking a bond between two carbon atoms.

With the recoil energy of 20 eV, we started to see more damage in the cellulose chains; in 39% of the simulations a broken D-glucose ring and also a number of free molecules were produced to the system: 7 water molecules and 13 radicals of the form OH and COH $_x$. Also 7% of the impacts broke a cellulose chain. Thus the threshold energy for breaking the glycosidic bond connecting the glucose units appears to be

Table II. Broken Chains, Broken D-Glucose Rings, Free Radicals/Saturated Molecules, and Cross-Links Formed in Cellulose in Single-Impact Simulations^a

E_{rec} [eV]	no. sims	broken chains	broken rings	free molecules	cross-links
10	100	0.0	0.05	0.0	0.0
20	100	0.07	0.39	0.20	0.0
30	100	0.25	0.56	0.34	0.0
50	100	0.36	0.65	0.85	0.0
100	100	0.63	1.1	1.4	0.01

^aHalf of the recoil atoms used in simulations are carbon and half are oxygen. The reported values are the average number of occurrences per simulation.

between 10 and 20 eV, that is, roughly twice as high as compared to the overall damage threshold. No cross-links were formed between cellulose chains.

In simulations with 30 eV of recoil energy we observed broken D-glucose rings in more than half of the simulations and a variety of free molecules: 1 H $_2$, 12 water molecules, and 21 radicals of form OH, CO, COH $_x$, and C $_2$ OH $_x$. The impacts with 30 eV of recoil energy broke the target chain in 25% of the occasions, but no cross-links were formed.

With the higher recoil energies of 50 and 100 eV, we observed broken chains in 36 and 63% of the cases, respectively. For 50-eV recoils, 65 broken rings were produced, and for 100-eV recoils, 114 broken rings were produced during 100 simulations. C recoils were more than twice as likely to produce broken rings than O recoils, which is to be expected, since the D-glucose ring has five carbons and one oxygen, and on average 83% of the C recoils hit the ring, whereas for the O recoils the hit percentage is only 20%.

A single case of cross-linking, shown in Figure 4, was observed as a result of one of the 100 eV recoils. The carbon

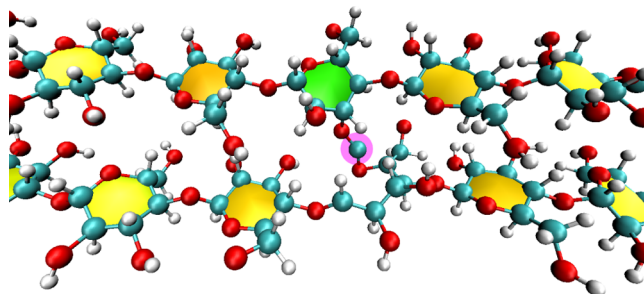


Figure 4. A cross-link formed between two cellulose chains as a result of a 100-eV C recoil. The figure shows only the atoms bonded with the two cross-linked chains.

atom highlighted with pink halo is the recoil atom that has traveled few nanometers from the original impact site, before breaking the glucose ring in the lower chain and forming a cross-link by bonding with oxygens from both chains.

The distribution of free radicals and molecules produced with recoil energies of 50 and 100 eV is shown in more detail in Figure 5. With a recoil energy of 50 eV the biggest group of free molecules was COH $_x$ radicals with an average of 0.31 occurrences per simulation, followed by OH $_x$ molecules with 0.29 (mostly water molecules, 0.24 per simulation). The third biggest group was molecular hydrogen with 0.15 molecules per simulation. With the recoil energy of 100 eV, molecular hydrogen was the most abundant type of free molecule with

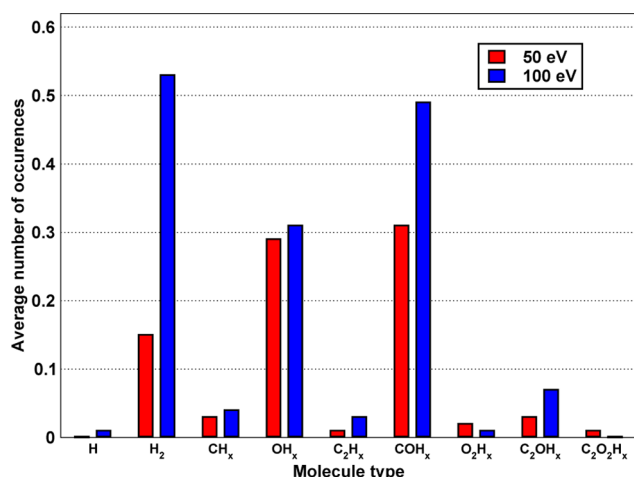


Figure 5. Average number of different types of free radicals and other molecules after the single-impact simulations of cellulose with 50- and 100-eV recoil energies. The molecule types are ordered by increasing molecular mass.

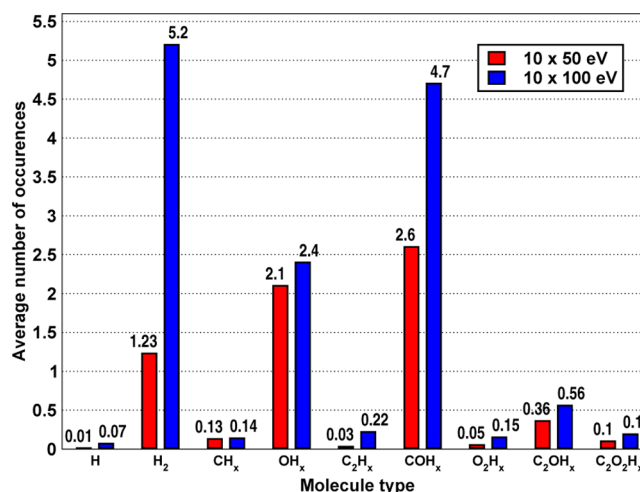


Figure 6. Average distribution of free radicals and other molecules in cellulose after 10 consecutive recoils with 50 eV (red bars) and 100 eV (blue bars) energy. The molecule types are ordered by increasing molecular mass.

0.53 per simulation. The close second were COH_x radicals with on average 0.49 per simulation.

The average amount of fragments (both radicals and nonreactive molecules) formed per 50-eV recoil is 0.85 and per 100-eV recoil is 1.4. These numbers represent the situation after the 20-ps simulation period. Immediately after the impact, there are about twice as many free fragments in the simulation system, on average 1.7 after 50-eV recoils and 3.2 after 100-eV recoils, but during the simulation period many of these combine into nonreactive molecules such as H₂ or H₂O or they form bonds with neighboring chains. This is in good agreement with experiments, where the number of radicals per dose of 100 eV in cellulose is estimated to be no higher than 4.⁸

Just as is the case with polyethylene, the formation of radicals occurs during the first 1 ps after the recoil and most of the recombination during the next 3 ps. The temperature of the system after 4 ps is cooled down to 25 K (100 eV recoils), and from there it decreases smoothly to 5 K by the end of the 20 ps simulation period. The shape of the temperature curve is identical to the polyethylene simulations, but the temperature values are about 50% higher. The temperature rise in irradiated materials is proportional to the absorbed dose and inversely proportional to the heat capacity.³ Since the heat capacity of HDPE is 2.3 J/g K³ and the heat capacity of 100% crystalline cellulose is about 1.2 J/g K,²⁸ we get $\Delta T_{\text{cellulose}}/\Delta T_{\text{PE}} \approx 1.6$, which is in good agreement with the simulation results.

With 50 or 100 eV of energy, the C and O recoils have mostly similar effects. For example, with 50-eV recoil energy the C recoils produces 43 free molecules and 22 broken chains, whereas O recoils produced 42 free molecules and 16 broken chains. The biggest differences were in the amounts of broken glucose rings. With 50-eV C recoils, 44 broken rings were formed, and with O recoils, 21. Similarly, 100-eV C recoils produced 65 broken chains, and O recoils produced 49.

Cumulative Bombardment. In cumulative bombardment, cellulose was exposed to 50- and 100-eV recoils, 100 simulation sets of 10 consecutive bombardments each were carried out with for both recoil energies, corresponding to a total radiation dose of 1.55 and 3.1 MGy, respectively.

Figure 6 illustrates the distribution of free radicals and saturated molecules formed after the cumulative bombardment.

As expected, multiple impacts result in more damage of the target than single impacts. More free radicals and molecules are produced inside the target although their chemical structure and mass distributions are very similar compared with the ones caused by single impacts.

Again, the most abundant molecules in the 50-eV simulations are COH_x radicals, and in 100-eV simulations the molecular hydrogens are the most abundant, with average amounts of 2.6 and 5.2 per simulation set. Also the second and third most abundant groups are the same for both recoil energies as they were in the single-impact simulations: OH_x and H₂ molecules for 50 eV; COH_x and OH_x for 100 eV. About 90% of the OH_x group consists of water molecules (1.9 of 2.1 for 50 eV recoils and 2.1 of 2.4 for 100 eV recoils).

Actually, all the free molecule abundances after cumulative bombardment, shown in Figure 6, are close to what one would get by just multiplying the single-impact values, shown in Figure 5, by ten. The total number of free molecules after the cumulative bombardment was 663 molecules with 50-eV recoils and 1362 molecules with 100-eV recoils. Both of these numbers are somewhat less than 10 times the number of free molecules after single-impact simulations, 85 and 150, respectively. This is to be expected since the possible pre-existing damage around the recoil site during consecutive bombardment makes it more probable for the new radicals to form bonds with nearby reactive cellulose chains or free radicals.

After the 10 consecutive recoils, there were on average 2.9 broken cellulose chains per simulation set in the 50-eV systems and in the 100-eV systems on average 4.3 broken chains. Thus the number of broken chains caused by one recoil event in cumulative bombardment (0.29 with 50 eV and 0.43 with 100 eV) is less than the number of broken chains (0.36 and 0.63) in single-impact simulations. Again, this is to be expected, since part of the consecutive recoil impacts hit into chains already broken by previous impacts, and it also probable that on some occasions the longer simulation time allows for previously broken chains to mend.

Cross-linking was observed in 5% of the 50-eV recoil simulation systems and in 32% of the 100-eV systems. The total number of cross-links in the 50-eV systems was 6, meaning 0.6% probability for cross-linking per single recoil event. In the

100-eV systems, a total of 41 cross-links were formed, meaning cross-links were formed as a result of 4.1% of recoil events.

Discussion. In both polyethylene and cellulose, we found the occurrence probability of cross-linking to be small. In 100-eV polyethylene simulations, we observed 0.02 ± 0.014 cross-links per recoil event in single-impact simulations and 0.02 ± 0.004 cross-links per recoil event in cumulative bombardment simulations. Thus it seems that consecutive bombardments do not increase the probability for cross-linking in polyethylene or at least the change is within the margin of error. In cellulose simulations using 100 eV recoil energy, we observed 0.01 ± 0.01 cross-links per recoil event in single-impact simulations, and after cumulative bombardment, we observed 0.041 ± 0.006 cross-links per recoil event. Thus it seems that cross-linking is more probable when irradiating cellulose sample with previous radiation damage.

The amount of free radicals and molecules produced during the irradiation was somewhat bigger in polyethylene; on average 19 free molecules were produced in HDPE as a result of the cumulative bombardment vs on average 14 free molecules in cellulose. This difference comes mostly from the lack of free hydrogens in the cellulose systems, almost all of the free hydrogens produced by the recoil impacts bond with the other free radicals of the system or into other reactive chains. It is also worth bearing in mind that different version of the REBO potential was used in polyethylene and in cellulose simulations (see the Methods section for more details).

In cellulose simulations, we found that a broken glucose ring, similar to the one shown in Figure 3, was the most common type of radiation damage. Observing the simulation trajectories we found that this kind of damage seems to be well-protected from interaction by the rigid structure of the cellulose chain; even when the chain breaks, the large glucose units surrounding the damaged area usually prevent reactive atoms from interacting with the neighboring chains.

One of the reasons for the low occurrence of cross-linking is that the simulated phases of both materials were pure crystals. It has been observed that irradiation sufficient to cause appreciable cross-linking at ambient temperature in the amorphous phase of polymeric materials (like in the case of polyethylene) produces only a little change in the crystal phase.²⁹ Instead it seems that, according to experiments, cross-linking in the amorphous phase is more probable because of already existing disorder and irregularity among the polymer chains.³⁰ For instance the level of cross-linking within crystalline regions of HDPE has been reported to be about one-fourth of that in amorphous regions.¹¹

It has also been observed by Lawton et al.³¹ that radicals generated upon irradiation are trapped in the crystalline region of polyethylene. The lifetime of these is many times longer relative to radicals in the amorphous region. This indicates that radicals in the crystal phase have low diffusion rates and the role of radical diffusion is thus small for the cross-linking reaction. However, quick heating of the samples near to their melting point has been observed to increase cross-linking in both crystalline and amorphous phases, in the case of polyethylene.³¹

Simulation of amorphization by annealing polymeric materials is nonetheless problematic. For example, annealing the polyethylene system described earlier at a temperature of 500 K for 50 ps did not result in any amorphization, while experimentally the melting point for polyethylene is found to be around 400–450 K. The likely reason for this is that the simulation time is too short for the phase transition to occur.

Another reason is that periodic boundary conditions are applied, so that no nucleation site for the phase transition, such as a surface, is provided. Indeed it has been reported that hard materials can, in absence of a surface, be superheated by ~20% before they melt.³²

The low occurrence of cross-linking may also partly be a time scale issue. It has been suggested that the mechanism of cross-linking of polymers is due to radical–radical reactions in the seconds time domain.¹² The longest time scales realistically achievable in MD simulations of the kind performed in this work are a few nanoseconds, and it is possible that a significant part of the cross-linking occurs in longer time scales than that. For example, according to J. K. Thomas,¹² after radiolysis of polyethylene containing 10^{-2} of pyrene, it can take about 5 ms for all excited states and ions to decay.

CONCLUSIONS

The irradiation effects on HDPE and cellulose I β have been determined using atomistic simulations to better understand the reactions that occur in these materials and to obtain insight into the mechanism of cross-linking. For both materials both single and cumulative impact simulations were carried out.

In both materials, chain scission was observed to be the most common reaction. The number of free molecules increased in both materials with increasing recoil energy, the most common group of molecules being atomic and molecular hydrogen in HDPE, and molecular hydrogen and radicals of form COH_x in cellulose.

Crystalline cellulose was found to be more resistant to radiation damage than crystalline polyethylene. This appears to be mostly a sterical effect: the size of the glucose units protects the chains from chain scission, and the rigid structure of the crystal prevents the reactive sites from interacting with neighboring chains. In consecutive bombardment simulations, where the sample is damaged by previous recoil impacts, the occurrence of cross-linking increased.

AUTHOR INFORMATION

Corresponding Author

*E-mail: jussi.polvi@helsinki.fi.

Notes

The authors declare no competing financial interest.

ACKNOWLEDGMENTS

This work was performed within the Finnish Centre of Excellence in Computational Molecular Science (CMS), financed by The Academy of Finland and the University of Helsinki. Grants of computer time from CSC IT Center for Science Ltd. in Espoo, Finland, are gratefully acknowledged. T.W.K. and S.B.S. gratefully acknowledge the support of the National Science Foundation (Grant No. CHE-0809376). T.J. acknowledges support from the Academy of Finland (project 136165). J.P. also acknowledges funding from the SMART-WOOD project.

REFERENCES

- (1) Gould, R. F. *Irradiation of Polymers*; American Chemical Society: Washington, D.C., 1967.
- (2) Przybytniak, G.; Nowicki, A. *NUKLEONIKA* **2008**, *53* (Suppl.2), s67–s72.
- (3) Cleland, M. R.; Parks, L. A.; Cheng, S. *Nucl. Instr. Meth. Phys. Res. B* **2003**, *208*, 66–73.
- (4) Gehring, J.; Zyball, A. *Radiat. Phys. Chem.* **1995**, *46*, 931–936.

- (5) Patel, G. N.; Keller, A. J. *Polym. Sci.: Polym. Phys.* **1975**, *13*, 303–321.
- (6) Heiner, A. P.; Sugiyama, J.; Teleman, O. *Carbohydr. Res.* **1995**, *273*, 207–223.
- (7) Driscoll, M. *Radiat. Phys. Chem.* **2009**, *78*, 539–542.
- (8) Kovalev, G. V.; Bugaenko, L. T. *High Energy Chem.* **2003**, *37*, 209–215.
- (9) Charlesby, A. *Atomic radiation and polymers*; Pergamon Press Inc., 1960.
- (10) Chapiro, A. *Radiat. Res. Suppl.* **1964**, *4*, 179–191.
- (11) Singh, A. *Radiat. Phys. Chem.* **1999**, *56*, 7556–7570.
- (12) Thomas, J. K. *Nucl. Instr. Meth. B* **2007**, *265*, 1–7.
- (13) Perez, C. J. *Radiat. Phys. Chem.* **2010**, *79*, 710–717.
- (14) Beardmore, K. *Nucl. Instr. Meth. B* **1995**, *102*, 223–227.
- (15) Takács, E.; Wojnárovits, L.; Borsa, J.; Fodváry, C.; Hargittai, P.; Zold, O. *Radiat. Phys. Chem.* **1999**, *55*, 663–666.
- (16) Wencka, M.; Wichlacz, K.; Kasprzyk, H.; Lijewski, S.; Hoffmann, S. K. *Cellulose* **2007**, *14*, 183–194.
- (17) Desmet, G.; Takács, E.; Wojnárovits, L.; Borsa, J. *Radiat. Phys. Chem.* **2011**, *80*, 1358–1362.
- (18) Allen, M. P.; Tildesley, D. J. *Computer Simulation of Liquids*; Oxford University Press: Oxford, England, 1989.
- (19) Nordlund, K. 2006, parcas computer code. The main principles of the molecular dynamics algorithms are presented in refs 33 and 34. The adaptive time step and electronic stopping algorithms are the same as in ref 35.
- (20) Stuart, S. J. *J. Chem. Phys.* **2000**, *112*, 6472–6486.
- (21) Brenner, D. W.; Shenderova, O. A.; Harrison, J. A.; Stewart, S. J.; Ni, B.; Sinnott, S. B. *J. Phys.: Condens. Matter* **2002**, *14*, 783–802.
- (22) Brenner, D. W. *Phys. Rev. B* **1990**, *42*, 9459–9471.
- (23) Ni, B.; Lee, K.-H.; Sinnott, S. B. *J. Phys.: Condens. Matter* **2004**, *16*, 7261–7275.
- (24) Kemper, T.; Sinnott, S. B. *Plasma Processes Polym.* **2012**, *9*, 690–700.
- (25) Berendsen, H. J. C.; Postma, J. P. M.; van Gunsteren, W. F.; DiNola, A.; Haak, J. R. *J. Chem. Phys.* **1984**, *81*, 3684–3690.
- (26) Egerton, R. F.; Li, P.; Malac, M. *Micron* **2004**, *35*, 399–409.
- (27) Yoshiharu, N. *J. Am. Chem. Soc.* **2002**, *124*, 9074–9082.
- (28) Hatakeyama, T.; Hatakeyama, H. *Thermal properties of green polymers and biocomposites*; Kluwer Academic Publishers: Dordrecht, Netherlands, 2004.
- (29) Adler, G. *Science* **1962**, *141*, 321–329.
- (30) Singh, A. *Radiat. Phys. Chem.* **2001**, *60*, 453–459.
- (31) Lawton, E. J.; Balwit, J. S.; Powell, R. S. *J. Polym. Sci.* **1958**, *32*, 257–275.
- (32) Nordlund, K.; Ghaly, M.; Averbach, R. S.; Caturla, M.; de la Rubia, T. D.; Tarus, J. *Phys. Rev. B* **1998**, *57*, 7556–7570.
- (33) Nordlund, K.; Ghaly, M.; Averbach, R. S.; Caturla, M.; Diaz de la Rubia, T.; Tarus, J. *Phys. Rev. B* **1998**, *57*, 7556–7570.
- (34) Ghaly, M.; Nordlund, K.; Averbach, R. S. *Phil. Mag. A* **1999**, *79*, 795.
- (35) Nordlund, K. *Comput. Mater. Sci.* **1995**, *3*, 448.